Detailed Characterization of the Cooperative Mechanism of Ca^{2+} Binding and Catalytic Activation in the Ca^{2+} Transport (SERCA) ATPase†

Zhongsen Zhang, David Lewis, Christopher Strock, and Giuseppe Inesi*

Department of Biochemistry and Molecular Biology, University of Maryland School of Medicine, Baltimore, Maryland 21201

Masayoshi Nakasako, Hiromi Nomura, and Chikashi Toyoshima

Institute of Molecular and Cellular Biosciences, The University of Tokyo, Bunkyo-ku, Tokyo 113, Japan

Received January 31, 2000; Revised Manuscript Received March 29, 2000

ABSTRACT: Expression of heterologous SERCA1a ATPase in Cos-1 cells was optimized to yield levels that account for 10−15% of the microsomal protein, as revealed by protein staining on electrophoretic gels. This high level of expression significantly improved our characterization of mutants, including direct measurements of Ca^{2+} binding by the ATPase in the absence of ATP, and measurements of various enzyme functions in the presence of ATP or P_i. Mutational analysis distinguished two groups of amino acids within the transmembrane domain: The first group includes Glu771 (M5), Thr799 (M6), Asp800 (M6), and Glu908 (M8), whose individual mutations totally inhibit binding of the two Ca^{2+} required for activation of one ATPase molecule. The second group includes Glu309 (M4) and Asn796 (M6), whose individual or combined mutations inhibit binding of only one and the same Ca^{2+}. The effects of mutations of these amino acids were interpreted in the light of recent information on the ATPase high-resolution structure, explaining the mechanism of Ca^{2+} binding and catalytic activation in terms of two cooperative sites. The Glu771, Thr799, and Asp800 side chains contribute prominently to site 1, together with less prominent contributions by Asn768 and Glu908. The Glu309, Asn796, and Asp800 side chains, as well as the Ala305 (and possibly Val304 and Ile307) carbonyl oxygen, contribute to site 2. Sequential binding begins with Ca^{2+} occupancy of site 1, followed by transition to a conformation (E′) sensitive to Ca^{2+} inhibition of enzyme phosphorylation by P_i, but still unable to utilize ATP. The E′ conformation accepts the second Ca^{2+} on site 2, producing then a conformation (E″) which is able to utilize ATP. Mutations of residues (Asp813 and Asp818) in the M6/M7 loop reduce Ca^{2+} affinity and catalytic turnover, suggesting a strong influence of this loop on the correct positioning of the M6 helix. Mutation of Asp351 (at the catalytic site within the cytosolic domain) produces total inhibition of ATP utilization and enzyme phosphorylation by P_i, without a significant effect on Ca^{2+} binding.

The catalytic and transport cycle of SERCA[1] ATPases begins with cooperative and high-affinity binding of two Ca^{2+} per ATPase molecule, whereby the enzyme is shifted from an inactive to an activated state (E1). The active enzyme can then form a phosphorylated intermediate with the terminal phosphate of ATP. The phosphorylation reaction places the enzyme in a state (E2) that favors vectorial displacement of the two bound Ca^{2+}, followed by hydrolytic cleavage of P_i (for reviews, see refs *1*−*4*). The topology of these partial reactions within the ATPase protein is very important to our understanding of the catalytic and transport mechanism. It is known, in this regard, that the ATP binding and phosphorylation domains reside within the cytosolic region of the ATPase (*5*). On the other hand, experiments on site-directed mutagenesis suggest that several residues within the membrane-bound region (Figure 1) are involved in Ca^{2+} binding (*6*). Information on the topology of these domains within the ATPase molecule has been recently obtained by cryoelectron microscopy (*7*−*10*) and X-ray diffraction (*11*).

The suggestion that the Ca^{2+} binding domain resides within the membrane-bound region of the ATPase was originally based on the interference of single mutations with the normally observed Ca^{2+} inhibition of reverse enzyme phosphorylation by P_i. However, direct measurements of Ca^{2+} binding (or lack thereof) by these mutants were prevented by the low transfection efficiency and the limited quantities of recombinant protein obtained from cell cultures. Therefore, it was impossible to distinguish whether the observed mutational effects were due to direct inhibition of Ca^{2+} binding, or to interference with the mechanism of Ca^{2+} signaling.

† This work was supported by the U.S. National Institutes of Health (Program Project HL27867) and by Grants-in-Aid for Scientific Research and for International Scientific Research from the Ministry of Education, Science, Sports and Culture of Japan.

* Corresponding author. Telephone: 410-706-3220. Fax: 410-706-8297. E-mail: ginesi@umaryland.edu.

[1] Abbreviations: SR, sarcoplasmic reticulum; SERCA, sarco(endo)-plasmic reticulum Ca^{2+}-ATPase; WT, wild type; ATP, adenosine 5′-triphosphate; BSA, bovine serum albumin; DMF, *N*,*N*-dimethylformamide; EGTA, ethylene glycol bis(β-aminoethyl ether)-*N*,*N*,*N*′,*N*′-tetraacetic acid; FBS, fetal bovine serum; LDS, lithium dodecyl sulfate; MOPS, 3-(*N*-morpholino)propanesulfonic acid; Mes, 2-(*N*-morpholino)-ethanesulfonic acid; Me_2SO, dimethyl sulfoxide; PCA, perchloric acid.

10.1021/bi000185m CCC: $19.00
Published on Web 07/06/2000

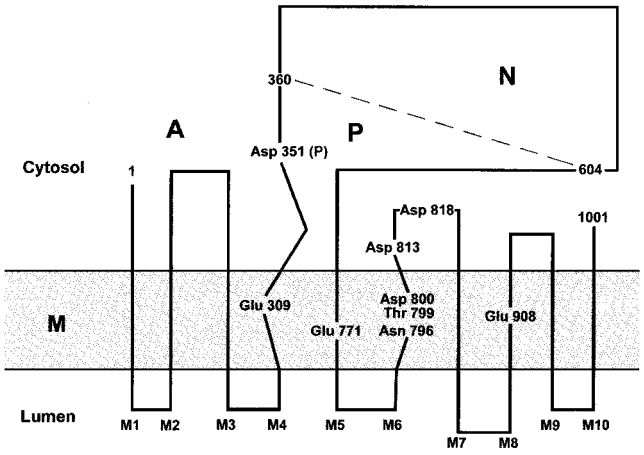

FIGURE 1: Topologic distribution of the SERCA amino acid sequence. The two-dimensional model of the SERCA1 protein is according to MacLennan et al. (*5*). The cytosolic sequence is divided in three sections (A: amino terminus; P: phosphorylation; N: nucleotide binding) yielding distinct regions in the folded structure (*11*). The residues subjected to mutational analysis in this study are indicated in the diagram. Asp351 resides in the catalytic site, within the cytosolic region. Glu309 is in transmembrane helix M4, Glu771 in M5, Asn796, Thr799, and Asp800 in M6, and Glu908 in M8. Asp813 and Asp818 reside within the M6/M7 loop. Interruptions of helical folding are represented in M4 and M6.

It was subsequently found that transfer of heterologous cDNA and expression of recombinant protein can be made much more efficient by the use of recombinant adenovirus vectors (*12*), thereby rendering possible preliminary measurements of Ca^{2+} binding (*13*). However, the accuracy of the measurements performed in a few mutants was still limited by an unfavorable signal-to-noise ratio. We now find that expression of recombinant SERCA1 ATPase in Cos-1 cells can be further increased by placing the cDNA construct under control of the CMV (rather than SV40) promoter in the adenovirus vector. Such high levels of recombinant ATPase allow measurements of Ca^{2+} binding by radioactive isotope tracer and filtration methods in the presence of Ca-EGTA buffers for control of free Ca^{2+}, using microsomes obtained from infected cells directly, with no need for enzyme purification using detergents. We were able to perform detailed measurements of Ca^{2+} binding in the absence of ATP, and of catalytic functions in the presence of ATP or P_i, on previously reported as well as on new mutants (Figure 1). These advances, as well as recent information on the high-resolution structure of the ATPase (*11*), allowed us to clarify the role of various amino acid residues and structural ATPase segments in the mechanism of Ca^{2+} binding and catalytic activation.

METHODS

DNA Constructs and Vectors. The chicken fast twitch skeletal muscle SR (SERCA-1) ATPase cDNA (*14*) was inserted into the pUC19 plasmid for amplification, and then subcloned into the pSELECT-1 vector for site-directed mutagenesis. This was carried out by the Altered Sites In Vitro Mutagenesis System made available by Promega (Madison, WI), or by overlap extension using the polymerase chain reaction (*15*). A *c-myc* tag was added to the 3′ end to monitor ATPase expression using anti-*c-myc* antibodies, independently of mutations in the enzyme sequence.

Wild-type and mutated cDNA was subcloned into the shuttle plasmid pΔE1sp1A (Microbix BioSystems). In the final constructs, the cDNA was preceded by the SV40 or the CMV promoter, and followed by the SV40 polyadenylation signal, both obtained from the mammalian expression plasmid pCDL-SRα296 (*16*). The shuttle plasmids were either used directly for transfection of COS-1 cells by the DEAE-dextran method, or used for cotransfection of HEK293 cells in conjunction with the replication-defective adenovirus plasmid pJM17 (Microbix BioSystems) to obtain recombinant adenovirus vectors (*17*). The shuttle vector was constructed such that homologous recombination would result in an antisense direction of the SERCA cDNA with respect to the original adenovirus E1 gene and its promoter.

Alternatively, cDNA constructs were subcloned into pAd-*lox* shuttle vector and cotransfected with purified ψ5 adenovirus genome in CRE8 cells derived from the HEK293 line. CRE8 cells constitutively express the Cre recombinase, which catalyzes efficient recombination between loxP sites in the ψ5 genome and in the pAd-*lox* to yield recombinant adenovirus (*18*).

The recombinant products were plaque-purified and cesium-banded, yielding concentrations on the order of 10^{10} pfu/mL.

Cell Cultures and Transfections. Cultures of HEK293, CRE8, and COS-1 cells were maintained as described by Graham and Prevec (*17*), Hardy et al. (*18*), and Sumbilla et al. (*19*), respectively. The growth medium for COS-1 and Cre 8 cells was Gibco Dulbecco Modified Eagle Medium (DMEM) supplemented with 10% FBS (Gibco) and containing Penn-Strep (100 units/mL) and Fungizone (1 μg/mL). Modified Eagle Medium (MEM) was used for HEK293 cells.

Transfections of COS-1 cells with wild-type or mutated SERCA-1 cDNA, subcloned into the shuttle vector pΔE1sp1A or pAd-*lox*, were conducted by the DEAE-dextran method as described by Sumbilla et al. (*19*).

Recombinant adenovirus vectors were used as follows: 6 or 15 cm diameter plates of COS-1 cells (75−80% confluence) were aspirated to remove growth medium. The cells were then layered with 1 or 5 mL of infection medium (DMEM supplemented with 5% Horse Serum, 100 units of Penn-Strep/mL, and 1 μg of Fungizone/mL) containing 1.4×10^7 pfu/mL and corresponding to about 10 pfu/cell. One hour after infection, 4 or 20 mL of growth medium was added, and 48−60 h later, the cells were harvested for fluorescence microscopy with or without immunostaining, and for microsomal preparations.

Microsome Preparation and Immunodetection of Expressed Protein. The procedure for microsome preparation from infected COS-1 cells was as described by Autry and Jones (*20*), and the final product was stored in small aliquots at −70 °C. The total microsomal protein was determined using bicinchoninic acid with the biuret reaction (Pierce). The expressed SERCA-1 ATPase was detected by Western blotting. For this purpose, microsomal proteins were separated in 7.5% Laemmli (*21*) electrophoretic gels and blotted onto nitrocellulose paper. The blots were then incubated with a monoclonal antibody (mAb CaF3-5C3) to the chicken SERCA-1, and in parallel with a monoclonal antibody (mAb 9E10) to the *c-myc* epitope. After incubation with secondary antibody (goat anti-mouse IgG−horseradish peroxidase-conjugated), the bound proteins were probed using an

Enhanced Chemiluminescence-linked detection system (Amersham Corp.). Quantitation of immunoreactivity was obtained by densitometry, and standardized with samples of wild-type ATPase to be used as controls for the functional studies.

Sarcoplasmic reticulum microsomal vesicles were obtained from rabbit skeletal muscle according to Eletr and Inesi (*22*).

Functional Studies. ATPase hydrolytic activity was assessed by measuring P_i production (*23*). The reaction mixture contained 20 mM MOPS, pH 6.8, 80 mM KCl, 5.0 mM $MgCl_2$, 5 mM sodium azide, 1.0 mM EGTA, and $CaCl_2$ to yield various free Ca^{2+} concentrations, 10−30 μg of microsomal protein, and 3 μM A23187 Ca^{2+} ionophore. The reaction was started by addition of 1.0 mM ATP, and run at 37 °C. Serial samples were taken every 3 min for 15−20 min. Due to the presence of the Ca^{2+} ionophore, the ATPase reaction proceeded at constant velocity, yielding linear plots of P_i production.

Formation of phosphorylated intermediate by utilization of ATP was obtained in the presence of 20 mM MOPS, pH 6.8, 80 mM KCl, 5 mM $MgCl_2$, 30 μg of microsomal protein, variable Ca^{2+}, and 10.0 μM [γ-^{32}P]ATP, in a total volume of 250 μL. The reaction was started by the addition of ATP, run for 10 s at 2−3 °C temperature, and quenched by the addition of 1.0 mL of cold 1.0 M PCA. Rapid mixing upon addition of ATP and PCA was obtained by vortexing. The reagents were precooled in ice. The quenched samples were transferred into a 1.7 mL Eppendorf tube containing 100 μg of BSA as carrier protein, and placed in ice. The samples were then spun in a refrigerated clinical centrifuge at 3000 rpm for 5 min, and the sediments were washed 3 times with 1.0 mL of cold 0.125 M PCA and once with cold water. The final pellets were dissolved in 50 μL of LDS denaturing buffer [50 mg of lithium dodecyl sulfate, 0.01 mL of 2-mercaptoethanol, and 0.05 mL of Weber−Osborn (*24*) buffer per milliliter] and 10 μL of tracking dye solution (1 mg of bromophenol blue and 0.3 g of sucrose per milliliter). The entire samples were then run on 6.5% acrylamide gels at pH 6.2, with a current limit of 100 milliamperes, at 15 °C. The radioactive phosphoenzyme was detected both by autoradiography and by digital acquisition of radioactive signal from the gels by phosphoimaging (Molecular Dynamics STORM 840).

Reverse enzyme phosphorylation by P_i was obtained by adding 30 μg of microsomal protein to 0.2 mL of reaction mixture containing 50.0 mM MesTris, pH 6.2, or 50.0 mM MOPS, pH 7.0, 10 mM $MgCl_2$, 20.0% Me_2SO, 2.0 mM EGTA, and 25−400 μM [^{32}P]P_i. Alternatively, the EGTA was omitted, and 10 μM, 100 μM, or 1.0 mM $CaCl_2$ was added. Following a 10 min incubation at 37 °C, 1.0 mL of 1.0 M ice-cold PCA was added, and the samples were transferred into a 1.7 mL Eppendorf tube containing 100 μg of BSA as a carrier protein, and placed in ice. Centrifugation, washing, electrophoresis, and detection of phosphoenzyme were then conducted as described above for enzyme phosphorylation with ATP.

For measurements of Ca^{2+} binding to recombinant ATPase, microsomes (0.8 mg of microsomal protein/mL) were suspended in ice-cold medium containing 20 mM MOPS, pH 6.8, 80 mM KCl, 5 mM $MgCl_2$, 0.1 mM EGTA, and 3.8 μL of Me_2SO/mL either without or with thapsigargin to yield a 7.0 μM concentration. After incubation in ice for 10 min, an equivalent volume of ice-cold medium containing 20 mM MOPS, pH 7.0, 80.0 mM KCl, 5.0 mM $MgCl_2$, and enough $^{45}Ca-CaCl_2$ to yield 3.0 μM free Ca^{2+} was then added. The mixture was kept in ice for 10 min, and then sonicated (10 s × 3) with the probe of a Kontes model 3000-cd microultrasonic cell disruptor at 2.5 setting. (This brief sonication improved the reproducibility of sampling by disrupting clumps of vesicles, but did not change the overall binding characteristics of any mutant.) Samples (0.75 mL each) were placed on a Millipore filter (HAWP 0.45 μm, 25 mm diameter) under suction for approximately 30 s. The vacuum was then turned off; the filter was blotted on a paper towel to remove excess moisture, folded, and inserted into a 7 mL scintillation vial. The filters were dissolved with 1 mL of DMF, scintillation fluid was added, and the radioactivity measured by scintillation counting. The measured Ca^{2+} binding levels were finally adjusted to compensate for slight variations of recombinant ATPase expression in various preparations, with reference to a wild-type preparation as indicated by Western blots. The difference between samples incubated in the absence and in the presence of thapsigargin was considered to be specific Ca^{2+} binding. The sensitivity of all mutants to thapsigargin was ascertained in separate experiments by checking its inhibition of phosphorylation with P_i.

Endogenous Ca^{2+} in the equilibration media was determined by titration with EGTA in the presence of 50 μM Arsenazo III, and recording differential light absorption changes (660 and 687 nm wavelengths) with a DW-2000 SLM-Aminco spectrophotometer.

RESULTS

Expression and Activity of Wild-Type SERCA1. We established previously that transfections of COS-1 cells by methods based on the use of calcium phosphate, DEAE-Dextran, or liposomes are only effective on a small percentage of cells in culture. Therefore, the overall expression of exogenous genes is quite limited, even though interaction of the SV40 promoter with T antigen triggers plasmid amplification. On the other hand, transfer of heterologous cDNA can be made much more efficient by the use of recombinant adenovirus vectors whereby the entire population of COS-1 cells is infected and larger quantities of recombinant ATPase are produced (*13*). We now find that plasmid amplification triggered by SV40 interaction with COS-1 cells T antigen does not occur when adenovirus vector is used. Therefore, protein expression is highly dependent on the promoter's own strength, and expression is higher when the CMV rather than the SV40 promoter is used (Figure 2).

The high levels of protein expressed under control of the CMV promoter can be evidenced not only by Western blots, but even by staining electrophoretic gels directly with Coomassie Blue. Comparison of electrophoretic bands and measurements of ATPase activity (in the presence of 10 μM Ca^{2+}) indicate that the microsomal fraction of infected COS-1 cells contains recombinant SERCA protein at a concentration approximately one-fourth as high as that of the endogenous ATPase found in rabbit skeletal muscle microsomes (Figure 3).

Expression and ATPase Activity of SERCA1 Mutants. In addition to wild-type cDNA, we subcloned several cDNA

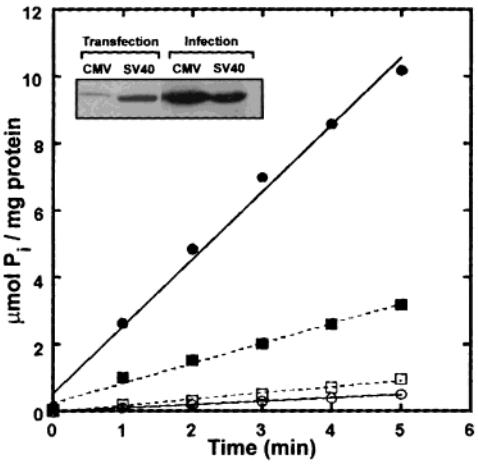

FIGURE 2: Ca^{2+} ATPase protein levels and activities in microsomes obtained from COS-1 cells transfected by the DEAE-Dextran method (○, □), or infected with adenovirus vectors (●, ■) carrying the SERCA cDNA under control of either the SV40 (■, □) or the CMV promoter (●, ○). Thapsigargin-sensitive ATPase was measured as described under Methods, in the presence of 10 μM Ca^{2+}. Western blots showing the amount of recombinant protein per unit weight of microsomal protein are reproduced in the inset.

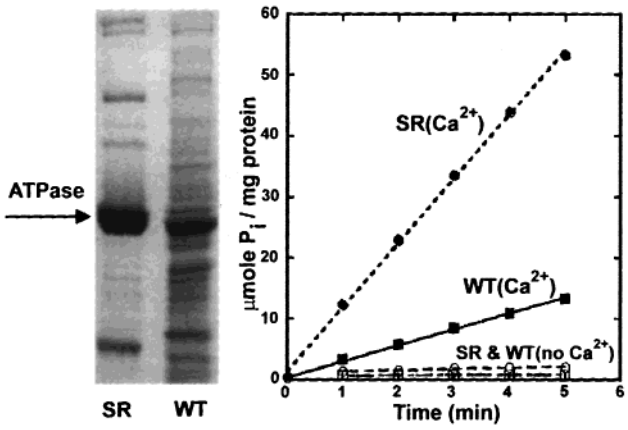

FIGURE 3: Protein composition and Ca^{2+} ATPase activity of rabbit SR and infected COS-1 cell microsomes. Equal amounts of microsomal fractions of rabbit skeletal muscle and of COS-1 cells infected with adenovirus vector containing wild-type SERCA1 cDNA, under control of the CMV promoter, were subjected to SDS gel electrophoresis and stained with Coomassie Blue. The right panel shows the Ca^{2+} (10 μM) dependent (●, ■) and Ca^{2+} independent (○, □) ATPase activity of microsomes obtained from rabbit muscle SR (●, ○), or from COS-1 cells infected with adenovirus containing WT SERCA1 cDNA under control of the CMV promoter (■, □).

mutants in adenovirus vectors, and obtained expression of SERCA1 mutants in infected COS-1 cells. As shown in Figure 1, the site-directed mutations were mostly produced within the coding sequences for the M4 (Glu309), M5 (Asp771), M6 (Asn796, Thr799, and Asp800), and M8 (Glu908) transmembrane segments, and included various side chain substitutions for the same amino acid, as well as double mutations. Additional mutations were produced within the M6/M7cytosolic loop (Asp813 and Asp818), and at the phosphorylation site (Asp351) within the cytosolic region. The expression levels were determined in all microsomal preparations by Western blots as well as by protein staining of electrophoretic gels. These levels were used to correct all functional parameters with reference to the same preparation of wild-type ATPase.

For a preliminary characterization of the functional consequences of mutations, we measured ATPase hydrolytic activity in the presence of 3.0 μM free Ca^{2+}, which is the concentration yielding maximal activation of the wild-type ATPase. It is shown in Table 1 that single mutations of Glu309 (M4) to Gln or Ala, Glu771 (M5) to Gln, Asn796 (M6) to Ala, Thr799 (M6) to Ala, and Asp800 (M6) to Asn produce very strong ATPase inhibition (cf. *6*, *25*−*27*). As expected on the basis of the effects of single mutations, we found that the double mutant Glu309Gln/Asn796Ala (M4 and M6) also produces strong inhibition of ATPase activity (Table 1). On the other hand, the Glu908Gln and Glu908Ala (M8) mutants retain 85% and 4% ATPase activity, respectively, in the presence of 3.0 μM Ca^{2+}.

It is also shown in Table 1 that the double mutants Asp813/Asn and Asp818/Asn (M6/M7 cytosolic loop) and the less conservative mutant Asp813Ala/Asp818Ala retain 43% and 28% ATPase activity, respectively, in the presence of 3 μM Ca^{2+} (Table 1). Finally we found that, as previously reported by Maruyama and MacLennan (*28*), a single mutation of Asp351 to Asn (cytosolic region) produces total loss of ATPase hydrolytic activity.

Ca^{2+} Binding in the Presence of 3 μM Free Ca^{2+}. The advantage of our expression system is that the microsomal fraction of infected COS-1 cells contains recombinant ATPase at concentrations permitting direct measurements of Ca^{2+} binding by isotopic tracer and filtration methods. In these new experiments, we were able to adjust the free Ca^{2+} concentration to the 3 μM level, which is the optimal concentration for saturation of the specific high-affinity sites of WT ATPase, with minimal involvement of nonspecific sites. We found that the specific (i.e., thapsigargin-sensitive) Ca^{2+} binding levels were 1.8−2.0 μmol/mg of microsomal protein of COS-1 cells expressing WT SERCA1 ATPase. These levels are approximately one-fourth of the Ca^{2+} binding obtained with native sarcoplasmic reticulum vesicles (8.0−9.0 μmol/mg of protein), which is consistent with the ATPase specific activity ratio of the two preparations. Therefore, the stoichiometry of Ca^{2+} binding by recombinant WT ATPase may be considered to be two calcium ions per ATPase molecule, as previously established for the native ATPase of sarcoplasmic reticulum ATPase (*29*).

It is shown in Table 1 that the Glu771Gln, Thr799Ala, and Asp800Asn mutations result in total loss of Ca^{2+} binding. This result indicates that a single, conservative mutation of any of these residues is sufficient to completely inhibit binding of both calcium ions, thereby indicating extensive interference with coordination geometry.

It was previously reported by Skerjanc et al. (*30*) that the Glu309Gln mutant retains binding of one (out of two) Ca^{2+} per ATPase, and that this was sufficient to inhibit the P_i reaction. This binding could be demonstrated only if the lumenal side of the membrane was exposed by the use of "E2" buffers and detergent treatment. In our experiments, conducted in the presence of 3 μM free Ca^{2+}, binding by this mutant is in fact 46% of that bound by the WT enzyme (Table 1); however, we do not find any requirement for "E2" buffer or detergent treatment. The finding that the less conservative mutation of Glu309 to Ala does not produce any additional reduction of Ca^{2+} binding (Table 1) demonstrates the specific role of the Glu309 acidic function.

Table 1: Effects of Various Mutations on Ca^{2+} Binding, ATPase Activity, Phosphoenzyme Formation by Utilization of ATP, and Ca^{2+} Inhibition of Enzyme Phosphorylation with P_i (pH 7.0)[a]

sample	ATPase activity	Ca^{2+} binding	EP (ATP)	EP (P_i) inhibn	group
$[Ca^{2+}] \rightarrow$	3 μM; 30 μM	3 μM	10 μM; 1 mM	10 μM; 1 mM	
WT	100; 100	100	100; 100	70; 100	−
D351N	ND; ND	97.5 ± 2.9	ND; ND	ND; ND	−
E309Q	ND; TR	45.7 ± 1.8	TR; TR	ND; 95	2
E309A	ND; TR	41.6 ± 0.2	TR; TR	ND; 80	2
N796A	ND; TR	54.7 ± 2.4	TR; TR	70; 100	2
E309Q/N796A	ND; ND	43.2 ± 1.8	ND; ND	50; 85	2
E771Q	ND; TR	ND	TR; 5	ND; ND	1
T799A	ND; ND	ND	ND; TR	ND; ND	1
D800N	ND; TR	ND	ND; TR	ND; ND	1
E908Q	85; 100	53.3 ± 5.3	100; 100	ND; 95	1
E908A	4; 8	ND	ND; ND	ND; ND	1
D813N/D818N	43; 57	43.4 ± 6.9	5; 10	20; 95	−
D813A/D818A	28; 45	16.5 ± 1.3	5; 8	ND; 90	−

[a] The Ca^{2+} concentrations in the reaction mixtures are indicated. ND = none detected; TR = traces. Numerical values are expressed as a percentage of maximal values observed with WT enzyme. Some residues (Glu771, Thr799, Asp800, and Glu908) are assigned to group 1 on the basis of total inhibition of Ca^{2+} binding produced by their mutations. Glu309 and Asn799 are assigned to group 2 on the basis of partial (only one Ca^{2+} out of two) of Ca^{2+} binding produced by their single or simultaneous mutations. Asp351, Asp813, and Asp818 were not assigned to any group either because their mutation did not inhibit Ca^{2+} binding, or their location in the ATPase structure precludes direct participation in Ca^{2+} binding.

It is of great interest that, in analogy to the Glu309Gln mutant, the Asn796Ala mutant retains 55% Ca^{2+} binding, and that the *double* Glu309Gln/Asn796Ala mutation still retains 43% binding (Table 1). This indicates that the effects of the Glu309 and Asn796 mutations are not additive, but are actually overlapping in their interference with only one (and the same) Ca^{2+}, out of the two Ca^{2+} bound by the wild-type ATPase.

At variance with the Glu309 mutations, the effects of Glu908 mutations are highly dependent on whether its carboxyl side chain is simply replaced by an amide or by a methyl group. In fact, the Glu908Gln mutant retains approximately 53% Ca^{2+} binding, while the Glu908Ala mutant produces total inhibition (Table 1). The effects of Asp813 and Asp818 double mutations (*31*) are also influenced by the more or less conservative nature of the replacement. In fact, the Asp813Asn/Asp818Asn mutant and the Asp813Ala/Asp818Ala mutant retain 43% and 16% Ca^{2+} binding, respectively. Finally, we found that the Asp351Asn mutant (cytosolic region) undergoes no significant reduction of Ca^{2+} binding, as compared to the wild-type enzyme (Table 1).

Ca^{2+} Concentration Dependence of the ATPase Activity. Previous studies have shown that several mutations displace the Ca^{2+} concentration dependence of functional parameters to a higher concentration range than that observed with wild-type enzyme (*32*−*34*). Unfortunately (even with rabbit sarcoplasmic reticulum vesicles), it is very difficult to obtain direct measurements of Ca^{2+} binding at high Ca^{2+} concentrations, due to the interference of nonspecific binding. Therefore, we sought to determine systematically the Ca^{2+} concentration dependence of functional parameters in our mutants, under conditions permitting comparative reference to our binding data.

It is shown in Figure 4A that, when WT ATPase is used, a 7−8-fold activation of catalytic activity occurs within the micromolar Ca^{2+} concentration range. On the other hand, activation of catalytic turnover is minimal with the Glu309Gln, Glu771Gln, Asn796Ala, Thr799Ala, and Asp800Asn mutants, even when the Ca^{2+} concentration is raised to 30 μM (Figure 4A,B).

The effects of Glu908 mutations are quite interesting inasmuch as it is possible to increase the activity of the conservative Glu908Gln mutant to the level of the WT ATPase, simply by raising the Ca^{2+} concentration 3-fold (Figure 4C). On the other hand, only very low activity is obtained with the Glu908Ala mutant, even when the Ca^{2+} concentration range is raised to 30 μM (Figure 4C; see also *25*). Raising the Ca^{2+} concentration is also effective in increasing the ATPase activity of the Asp813Asn/Asp818Asn and Asp813Ala/Asp818Ala double mutants (see also *31*). Even at high Ca^{2+}, however, the activity of these mutants is lower than that of the wild-type enzyme (Figure 4D). The ATPase activity observed with the Asp351Asn mutant in the presence of 1.0−30.0 μM Ca^{2+} was not significantly higher than that observed in the absence of Ca^{2+}.

Formation of Phosphorylated Enzyme Intermediate from ATP. The observations described above raise the question of whether, in any mutant, inhibition of ATPase activity is due to mutational interference with Ca^{2+} activation of the enzyme for formation of the phosphorylated enzyme intermediate, or with phosphoenzyme intermediate turnover. We therefore measured the steady-state levels of phosphoenzyme intermediate following addition of ATP to WT enzyme or mutants, in the presence of various concentrations of Ca^{2+}. No ATP utilization by WT ATPase was observed when Ca^{2+} was removed with EGTA (not shown), consistent with an absolute Ca^{2+} requirement for ATP utilization. Furthermore, while a strong phosphorylation signal was obtained with wild-type ATPase, no signal at all was observed with the Asp351Asn mutant, in agreement with the original finding (*35*, *36*) that Asp351 is the amino acid phosphorylated by ATP in the presence of Ca^{2+}.

It is shown in Figure 5 that the WT ATPase is phosphorylated by ATP to yield the same levels of phosphoenzyme at Ca^{2+} concentrations ranging from 10 μM to 1.0 mM. On the other hand, when the Glu309Gln, Glu771Gln, Asn796Ala, Thr799Ala, and Asp800Asn mutants are incubated with ATP in the presence of 10 μM Ca^{2+}, no significant phosphorylation (less than 1% as compared to WT ATPase) is observed. Very low levels of phosphorylation are obtained with these

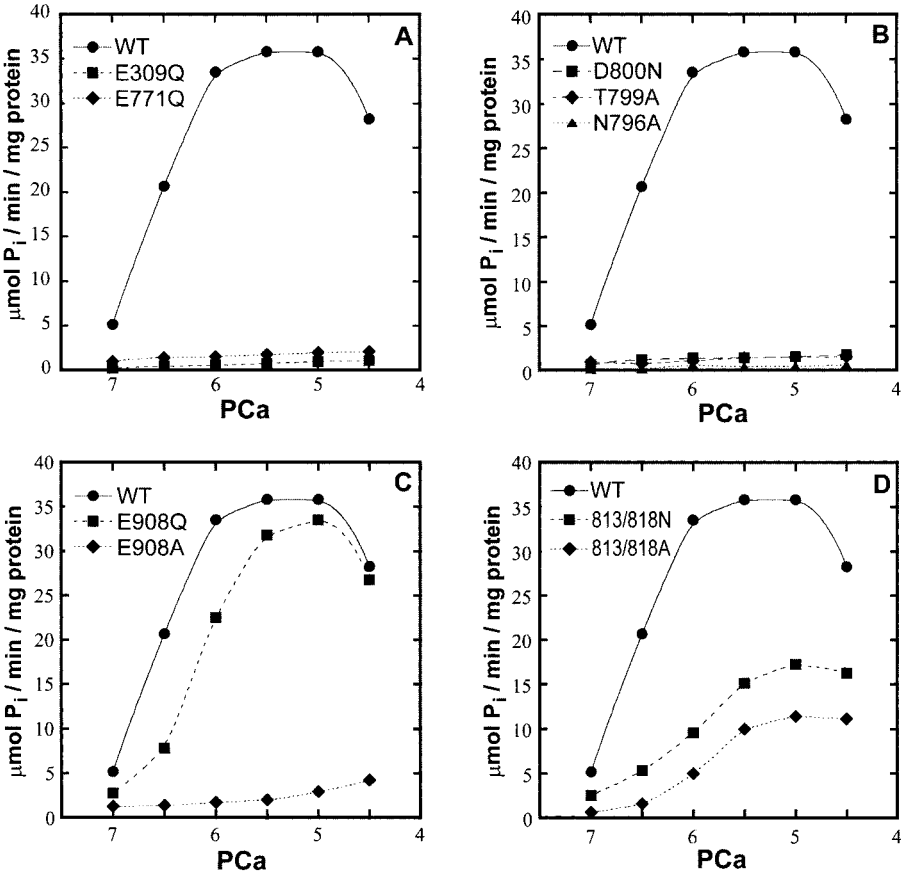

FIGURE 4: Ca^{2+} concentration dependence of ATPase activation. ATPase activity was followed by measuring P_i production in the presence of ATP, as described under Methods. The free Ca^{2+} concentration was regulated by EGTA-Ca buffers (*44*). Recombinant enzyme was obtained from COS-1 cells infected with adenovirus vectors carrying wild-type or mutated ATPase under control of the CMV promoter. The amount of microsomal protein added to the reaction mixture was adjusted to yield the same concentration of recombinant protein as revealed by Western blots.

mutants even if Ca^{2+} is raised to the millimolar level (see also *25*). These findings suggest that Ca^{2+} binding by these mutants is minimal even when the Ca^{2+} concentration is raised to the millimolar range. It should be understood that these measurements provide steady-state levels of the intermediate, as opposed to the equilibrium measurements obtained for Ca^{2+} binding and phosphorylation with P_i (see below). Therefore, due to higher rates of phosphoryl transfer from ATP as compared to phosphoenzyme hydrolytic cleavage, significant phosphoenzyme levels should be observed in steady state even when the equilibrium levels of Ca^{2+} binding in the absence of ATP are relatively low.

Consistent with the measurements of ATPase activity and Ca^{2+} binding, the Glu908Gln mutant yields nearly normal levels of phosphorylation, while low levels are obtained with the Glu908Ala and both Asp813/Asp818 mutants, even when the Ca^{2+} concentration is raised to the millimolar range (Figure 5).

Reverse ATPase Phosphorylation with P_i. SERCA ATPase can be phosphorylated by P_i in the reverse direction of the catalytic cycle. This reaction yields equilibrium levels of phosphoenzyme in the absence of Ca^{2+} and ATP, and at relatively high temperature (*37*). We found that, under our conditions, phosphorylation of WT enzyme and most mutants occurs with a K_d for P_i ranging between 33 and 40 μM, and maximal phosphoenzyme levels between 0.4 and 0.5 nmol/mg of microsomal protein. Considering that the recombinant ATPase content of microsomal protein is approximately 1 nmol/mg (i.e., 1.8−2.0 nmol of Ca^{2+} bound/mg), our levels of EP are consistent with an equilibrium constant ($EP/E{\cdot}P_i$) of approximately 1. The only exception is the Glu309Gln mutant, which requires the same P_i concentration range, but yields higher levels of phosphorylation (Figure 6). This is possibly due to a long-range effect of the Glu309 mutation in the transmembrane domain on the phosphorylation reaction in the cytosolic domain. It may be relevant in this regard that Adams et al. (*38*) reported enhancement of enzyme phosphorylation by P_i following mutation of Tyr295, which is in the M3-M4 loop on the lumenal side of the membrane.

It is noteworthy that we obtained no phosphorylation of the Asp351Asn mutant, in the absence or in the presence of Ca^{2+} (Figure 7). In fact, this is the first direct demonstration that enzyme phosphorylation by P_i in the absence of Ca^{2+} involves the same Asp351 residue which is phosphorylated by ATP in the presence of Ca^{2+}.

Interference with inhibition of the P_i reaction by Ca^{2+} was the original evidence suggesting Ca^{2+} binding defects in relevant mutants (*6*, *25*, *26*). We then performed a series of experiments to determine whether the characteristics of this reaction were affected by the mutations. It should be pointed out that under the conditions used, i.e., in the presence of Me_2SO, the Ca^{2+} concentration required to inhibit phosphorylation of WT ATPase (Figure 7) is somewhat higher (10.0 vs 3.0 μM) than observed under different conditions. We

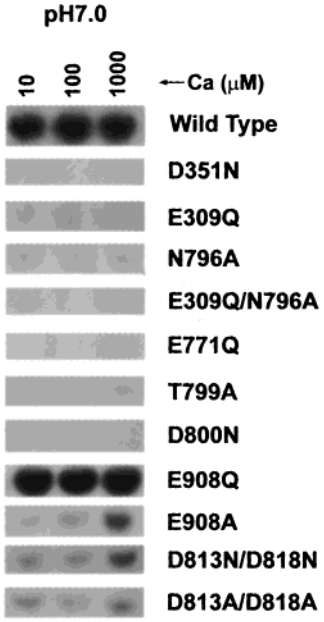

FIGURE 5: Formation of phosphorylated enzyme intermediate by utilization of ATP. Phosphoenzyme was obtained in the presence of ATP, and measured as described under Methods. Recombinant enzyme was obtained from COS-1 cells infected with adenovirus vectors carrying wild-type or mutated ATPase under control of the CMV promoter. The amount of microsomal protein added to the reaction mixture was adjusted to yield the same concentration of recombinant protein as revealed by Western blots. Therefore, the intensities of the bands are *proportional* to the phosphoenzyme levels obtained with equal amounts of recombinant protein. The three spots per each sample correspond to reactions performed in the presence of increasing Ca^{2+} concentrations: 10 μM, 100 μM, and 1 mM. No phosphoenzyme formation was observed removed with EGTA (not shown).

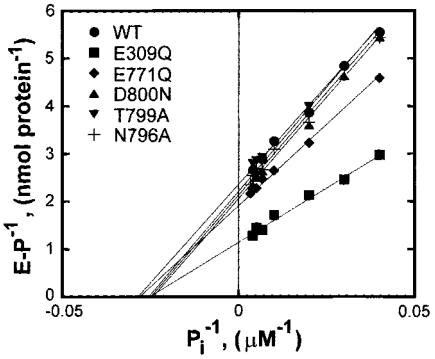

FIGURE 6: Phosphorylation of various mutants as a function of the P_i concentration. The phosphorylation reaction was carried out as described under Methods, in the absence of Ca^{2+} and in the presence of various P_i concentrations. Note that WT and mutant samples yield similar levels of phosphoenzyme, with the exception of Glu309Gln.

found that phosphorylation of the Glu771Gln, Thr799Ala, Asp800Asn, and Glu908Ala mutants still occurs even if the Ca^{2+} concentration is raised near the millimolar concentration range (Figure 7). This is consistent with total loss of specific Ca^{2+} binding (Table 1), as also indicated by the lack of ATPase activation over a wide range of Ca^{2+} concentrations (Figures 4A,B and 5). It should be pointed out that a precise analysis of the effect of high calcium on the phosphorylation levels may be somewhat limited by Ca^{2+} occupancy of sites other than the high-affinity specific sites. In fact, it was previously demonstrated that kinetic and equilibrium constants for the phosphorylation of native sarcoplasmic reticulum ATPase with P_i are influenced by divalent cations at relatively high concentrations (*39*).

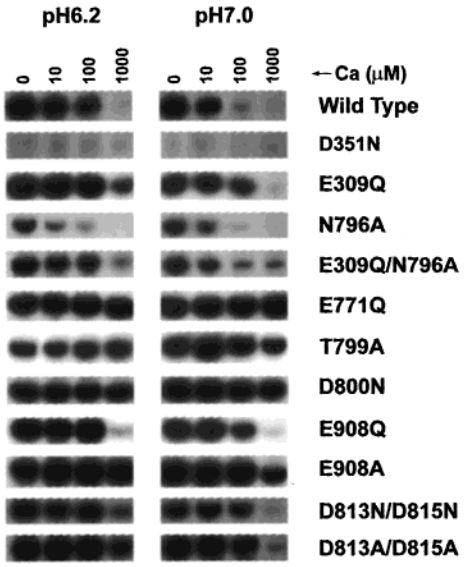

FIGURE 7: Enzyme phosphorylation with P_i, in the absence and in the presence of Ca^{2+}. The phosphorylation reaction was carried out as described under Methods, in the absence of Ca^{2+} (1 mM EGTA) or in the presence of 10 μM, 100 μM, or 1 mM Ca^{2+}, either at pH 6.2 or at pH 7.0. The autoradiogram film exposure was adjusted to render most evident the inhibitory effect of Ca^{2+} when present. Therefore, the intensities of the bands are *not proportional* to the phosphoenzyme levels obtained with equal amounts of recombinant protein. In fact, the phosphoenzyme levels were approximately equal for WT and mutants (except Glu309Gln) as shown in Figure 6.

It is shown in Figure 7 that the Asn796Ala and the Glu309Gln mutants manifest inhibition of the P_i reaction by 10−100 μM Ca^{2+}, even though binding only half as much Ca^{2+} as the WT ATPase. This finding suggests that these mutants bind only one Ca^{2+}, and that binding of this Ca^{2+} is sufficient to inhibit the P_i reaction (*25*). This conclusion is much strengthened by the fact that the simultaneous mutation of Glu309 to Gln and Asn796 to Ala does not produce additive effects, and phosphorylation of the double mutant is inhibited by Ca^{2+} equally well as phosphorylation of the single mutants. These experiments, viewed in the light of the calcium binding measurements, indicate that following individual or double mutations of the Glu309 and Asn796, the residual bound calcium is still able to inhibit ATPase phosphorylation by P_i. It is noteworthy that the sensitivity of the WT ATPase, and of those mutants that retain sensitivity to Ca^{2+}, is greater at pH 7.0 than at pH 6.2 (Figure 7). This behavior suggests that ionization of acidic residues participating in Ca^{2+} binding (e.g., Glu771, Asp800, and/or Glu908) occurs as the pH is shifted from 6.2 to 7.0, thereby facilitating binding of inhibitory Ca^{2+}. Ionization constants near neutral pH would facilitate Ca^{2+}/H^+ exchange.

Finally we found that, consistent with a reduced affinity of Ca^{2+} binding by the Asp813 and Asp818 mutants, inhibition of phosphorylation of these mutants with P_i requires millimolar Ca^{2+} (Figure 7).

DISCUSSION

The use of recombinant adenovirus vectors is of great advantage in obtaining heterologous SERCA expression in

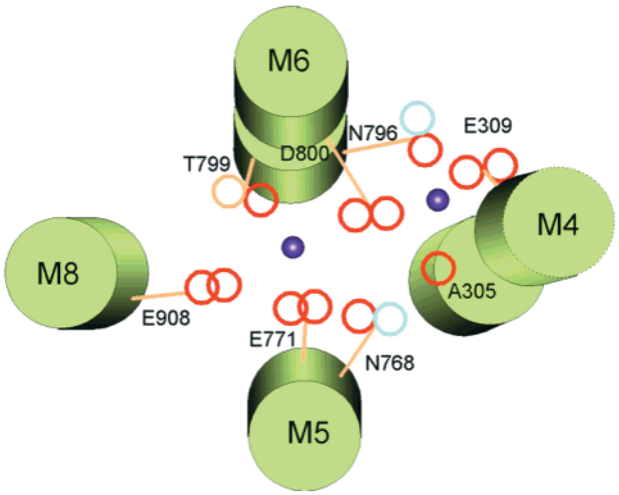

FIGURE 8: Diagram for the arrangement of transmembrane helices M4, M5, M6, and M8, and of the amino acids participating in Ca^{2+} binding. The arrangement is based on high-resolution X-ray crystallography of the enzyme with bound Ca^{2+} (*11*). The transmembrane helices are viewed from the cytoplasmic side roughly normal to the membrane. Note that M4 and M6 helices are unwound around E309 and D800 and two Ca^{2+} (blue spheres) are virtually at the same level. Oxygen atoms are shown as red circles, and nitrogen atoms as blue circles.

COS-1 cells under control of the CMV promoter. In fact, we obtained SERCA expression at levels that could be detected by direct Coomassie Blue staining of electrophoretic gels, showing that the recombinant protein accounts for 10−15% of the microsomal protein recovered from infected Cos-1 cells. These levels of recombinant ATPase improved significantly our ability to characterize the effects of mutations on the partial reactions of the catalytic cycle, including direct measurements of calcium binding in the presence of an EGTA-Ca^{2+} buffer for control of the free Ca^{2+} concentration.

Inspection of Table 1 shows clearly that the amino acid residues whose mutations interfere with high-affinity Ca^{2+} binding can be divided into two groups. Single mutations of residues in the first group interfere with binding of both Ca^{2+} known to bind to each WT ATPase molecule. On the other hand, single or even double mutations of amino acids in the second group affect only one and the same Ca^{2+} per ATPase, and therefore contribute to the same single site. In fact, if the effect of single mutations of Glu309 or Asn796 consisted of partial (~50%) inhibition of binding of both Ca^{2+}, simultaneous mutations of both these residues would yield additive effects and nearly total inhibition of Ca^{2+} binding. On the contrary, we did not observe any additive effect, indicating that single or double mutations of these residues interfere completely with binding of only one and the same Ca^{2+}.

It is noteworthy that the detailed structure obtained by X-ray crystallography (as represented by the diagram in Figure 8) indicates that interference of the first group mutations with binding of both Ca^{2+} is not necessarily due to direct coordination of both Ca^{2+} by the same amino acid. For example, single mutation of Thr799 affects drastically binding of both Ca^{2+}, even though this amino acid has only one side chain oxygen. It is therefore apparent that mutational disruption of one site can influence the other site through cooperative linkages.

Group 1 Residues. This group of residues includes Glu771 (M5), Thr799 (M6), and Asp800 (M6). Single mutations of amino acids in this group produce total interference with ATPase activity, Ca^{2+} binding, phosphoenzyme formation by utilization of ATP, and the inhibitory effect of Ca^{2+} on the P_i reaction. ATPase activity and inhibition of the P_i reaction by Ca^{2+} are not regained even if the Ca^{2+} concentration is raised to the millimolar range. Furthermore, structural analysis (Figure 8 and ref *11*) indicates that Glu908 and Asn768 also contribute to site 1, although conservative mutation of these residues produces only a reduction of Ca^{2+} affinity (Table 1, and *40*). Nevertheless, the important involvement of these residues, in the structure required for Ca^{2+} binding and catalytic activation, is demonstrated by the extensive effects of less conservative mutations (Table 1, and *40*).

Group 2 Residues. This group of residues includes Glu309 (M4) and Asn796 (M6), which are involved in binding one Ca^{2+}, without affecting binding of the alternate Ca^{2+}. The effects of mutations of group 2 residues are also characterized by (i) preservation of Ca^{2+} inhibition of the P_i reaction and (ii) complete inhibition of ATPase activity. This means that (i) inhibition of the P_i reaction requires binding of only one Ca^{2+} by group 1 residues, whereas (ii) activation of catalytic activity and utilization of ATP require binding of both Ca^{2+}. Therefore, elimination of Ca^{2+} binding by group 2 residues does not interfere with Ca^{2+} binding by the group 1 residues. On the other hand, rearrangement and stabilization of M4 through Ca^{2+} binding by group 2 residues are critical for activation of the catalytic site which is more than 30 Å distant. It should be stressed that Asn796 is on M6, and therefore classification of residues in group 1 or group 2 is not determined by the transmembrane segments that they belong to, but by their contribution to a particular Ca^{2+} site. Structural analysis indicates that one of the two Asp800 side chain oxygen atoms as well as the Ala305 (and possibly Val304 and Ile307) carbonyl oxygen also contribute to site 2 (Figure 8 and ref *11*).

Integration of Functional and Structural Data. Original measurements of Ca^{2+} binding in the absence of ATP (*29*) produced an equilibrium isotherm showing cooperative binding of 2 Ca^{2+} per mole of ATPase. The experimental points of the binding isotherm were fitted with a cooperative equation, derived from a sequential binding mechanism as in

$$E + Ca^{2+} \overset{1}{\leftrightarrow} ECa \overset{2}{\leftrightarrow} E'Ca + Ca^{2+} \overset{3}{\leftrightarrow} E''Ca_2$$

In this mechanism, binding of a first Ca^{2+} is followed by a slow isomeric transition, leading to the E′ conformation. The E′ conformation allows cooperative binding of the second Ca^{2+} and acquisition of the E″ conformation which is the activated enzyme state (generally known as E1). It was shown that the simulated time course of the slow isomer transition, based on the sequential mechanism, matches an experimentally determined rise of intrinsic tryptophan fluorescence, in parallel with enzyme activation (*41*). It was also shown (*42, 43*) that dissociation of both Ca^{2+} upon addition of EGTA is monophasic, while exchange of bound Ca^{2+} with medium calcium isotope is diphasic, suggesting cooperative stabilization of one bound Ca^{2+} by the other.

Mutational analysis (Table 1) demonstrates that Glu771, Thr799, and Glu800 are essential to the functional integrity of Ca^{2+} binding. Information derived from structural analysis shows (Figure 8) that these residues are mostly involved in coordination of a single Ca^{2+}, with participation of the Glu908 and Asn768 side chain oxygen atoms, and consequent rearrangement of the M5, M6, and M8 helices. Therefore, Ca^{2+} occupancy of the site formed by group 1 residues provides stabilization of the entire Ca^{2+} binding domain, and is required to trigger the isomeric transition predicted by the sequential binding equation.

The effects of the Glu309 (M4) and Asn796 (M6) single and double mutations demonstrate that these two residues are involved in binding the same Ca^{2+} at site 2. This is confirmed by structural studies (*11* and Figure 8) showing that suitable positioning of the Glu309 and Asn796 side chains is permitted by unwinding of the M4 and M6 helices. In addition, structural information indicates that one of the two oxygen atoms of the Asp800 side chain, as well as the carbonyl oxygen of Ala305 (and possibly of Val304 and Ile307), participates in binding. Disruption of this site can be produced by Glu309 and Asn796 mutations, without simultaneous disruption of Ca^{2+} binding by site 1 (Table 1). Most importantly, however, occupancy of site 2 and engagement of M4 are required to produce the E″ conformation and catalytic activation. The M4-S4 segment extends directly from the Ca^{2+} binding domain to the phosphorylation site (Figure 1), manifests marked homology to other cation transport ATPases, and is highly sensitive to mutations (*8*).

It should be pointed out that the side by side arrangement of the two Ca^{2+} shown in Figure 8 is not consistent with the stacking model that was originally suggested to explain the diphasic exchange of bound Ca^{2+} with medium Ca^{2+} (*43*). Therefore, the observed diphasic exchange is explained simply by the different binding constants (and inherent dissociation kinetics) of the two bound Ca^{2+}, produced by cooperative interactions of participating residues.

Role of the M6/M7 Loop. It was originally found by Menguy et al. (*34*) that double mutation of Asp813 and Asp818 to Ala in the cytosolic extension of M6 inhibits ATPase activity and displaces to a higher range the Ca^{2+} concentration required to form phosphoenzyme from ATP, and to inhibit the P_i reaction. This raised the possibility that these two residues might be involved in Ca^{2+} binding. We demonstrate here that Ca^{2+} binding is in fact reduced by mutation of Asp813 and Asp818 to Ala (Table 1). In addition, we mutated the same two residues to Asn, and found that a similar reduction of Ca^{2+} binding is produced by this conservative mutation as well. The string of aspartate residues in the M6-M7 loop is not positioned in the immediate vicinity of the transmembrane Ca^{2+} binding domain. Therefore, the effects of their mutations are not likely due to direct participation of these residues in Ca^{2+} binding.

It is possible to obtain phosphorylation of these mutants by ATP, as well as inhibition of the P_i reaction, if the Ca^{2+} concentration is increased. However, these mutants can regain their ability to utilize ATP only to approximately one-fourth of the WT level, even in the presence of millimolar Ca^{2+} (Figures 4D and 5). Therefore, mutations of the aspartate cluster in the M6/M7 loop interfere with activation of the catalytic mechanism, in addition to Ca^{2+} binding. It is of interest that mutations of neighboring prolines (811, 812, 820, and 821) also produce inhibition of ATPase activity, but do not reduce the enzyme affinity for Ca^{2+} (*34*). Therefore, the proline mutations offer an example of selective inhibition of catalytic activation by perturbation of the M6-7 loop. It is apparent that this loop plays an important role in linking Ca^{2+} binding to catalytic activation (Figures 1 and 8), presumably by influencing the arrangement of the M6 helix.

Role of Asp351. Complete catalytic inhibition is produced by conservative mutation of Asp351 to Asn, with no significant reduction of Ca^{2+} binding. Asp351 is the residue undergoing phosphorylation by utilization of ATP at the catalytic site in the cytosolic region of the ATPase. Our experiments show that simple substitution of the Asp351 carboxyl function with an amide interferes with the catalytic chemistry of ATP utilization, without long-range conformational effects on Ca^{2+} binding. It was previously demonstrated that the long-range effect on Ca^{2+} binding is triggered by phosphorylation of Asp351 with ATP or, more simply, by formation of a vanadate complex as a stable transition analogue of the phosphorylation reaction. Our findings demonstrate that while the Asp351 acidic function is required for the phosphorylation reaction to occur, it does not have by itself a direct influence on Ca^{2+} binding. It is rather the interaction of the phosphoryl moiety with neighboring residues which triggers destabilization of Ca^{2+} binding.

REFERENCES

1. de Meis, L., and Vianna, A. (1979) *Annu. Rev. Biochem. 48*, 275−292.
2. Inesi, G., Sumbilla, C., and Kirtley, M. E. (1990) *Physiol. Rev. 70*, 749−760.
3. Moller, J. V., Juul, B., and Le Maire, M. (1996) *Biochim. Biophys. Acta 1286*, 1−51.
4. MacLennan, D. H., Rice, W. J., and Green, N. M. (1997) *J. Biol. Chem. 272*, 28815−28818.
5. MacLennan, D. H., Brandl, C. J., Korczak, B., and Green, N. M. (1985) *Nature 316*, 696−700.
6. Clarke, D. M., Loo, T. W., Inesi, G., and MacLennan, D. H. (1989) *Nature 339*, 476−478.
7. Toyoshima, C., Sasabe, H., and Stokes, D. L. (1993) *Nature 362*, 469−471.
8. Zhang, Z., Sumbilla, C., Lewis, D., Summers, S., Klein, M. G., and Inesi, G. (1995) *J. Biol. Chem. 270*, 16283−16290.
9. Ogawa, H., Stokes, D. L., Sasabe, H., and Toyoshima, C. (1998) *Biophys. J. 75*, 41−52.
10. Stokes, D. L., Auer, M., Zhang, P., and Kuhlbrandt, W. (1999) *Curr. Biol. 9*, 672−679.
11. Toyoshima, C., Nakasako, M., Nomura, H., and Ogawa, H. (2000) *Nature* (in press).
12. Inesi, G., Lewis, D., Sumbilla, C., Nandi, A., Strock, C., Huff, K. W., Rogers, T. B., Johns, D. C., Kessler, P. D., and Ordahl, C. P. (1998) *Am. J. Physiol. 274*, C645−C653.
13. Strock, C., Cavagna, M., Peiffer, W., Sumbilla, C., Lewis, D., and Inesi, G. (1998) *J. Biol. Chem. 273*, 15104−15109.
14. Karin, N. J., Kaprielian, Z., and Fambrough, D. M. (1989) *Mol. Cell. Biol. 9*, 1978−1986.
15. Ho, S. N., Hunt, H. D., Horton, R. M., Pullen, J. K., and Pease, L. R. (1989) *Gene 77*, 51−59.
16. Takebe, Y., Seiki, M., Fujisawa, J. I., Hoy, P., Yokota, K., Arai, K. I., Yoshida, M., and Arai, N. (1988) *Mol. Cell. Biol. 8*, 466−472.
17. Graham, F. L., and Prevec, L. (1992) in *Vaccines: New approaches to immunological problems* (Ellis, R. W., Ed.) pp 363−390, Butterworth-Heinemann, Boston, MA.
18. Hardy, S., Kitamura, M., Harris-Stansil, T., Dai, Y., and Phipps, M. L. (1997) *J. Virol. 71*, 1842−1849.

19. Sumbilla, C., Lu, L., Inesi, G., Ishii, T., Takeyasu, K, Fang, Y., and Fambrough, D. M. (1993) *J. Biol. Chem. 268*, 21185−21192.
20. Autry, J. M., and Jones, L. R. (1997) *J. Biol. Chem. 272*, 15872−15880.
21. Laemmli, U. K. (1970) *Nature 227*, 680−685.
22. Eletr, S., and Inesi, G. (1972) *Biochim. Biophys. Acta 282*, 174−179.
23. Lanzetta, P. A., Alvarez, L. J., Reinsch, P. S., and Candia, O. A. (1979) *Anal. Biochem. 100*, 95−97.
24. Weber, K., and Osborn, M. (1969) *J. Biol. Chem. 244*, 4406−4417.
25. Andersen, J. P. (1995) *Biosci. Rep. 15*, 243−261, 1995.
26. Chen, L., Sumbilla, C., Lewis, D., Zhong, L., Strock, C., Kirtley, M. E., and Inesi, G. (1996) *J. Biol. Chem. 271*, 10745−10752.
27. Rice, W. J., Green, N. M., and MacLennan, D. H. (1997) *J. Biol. Chem. 272*, 31412−31419.
28. Maruyama, K., and MacLennan, D. H. (1988) *Proc. Natl. Acad. Sci. U.S.A. 85*, 3314−3318.
29. Inesi, G., Kurzmack, K., Coan, C., and Lewis, D. (1980) *J. Biol. Chem. 255*, 3025−3031.
30. Skerjanc, I. S., Toyofuku, T., Richardson, C., and MacLennan, D. H. (1993) *J. Biol. Chem. 268*, 15944−15950.
31. Falson, P., Menguy, T., Corre, F., Bouneau, L., De Gracia, A. G., Soulié, S., Centeno, F., Moller, J. V., Champeil, P., and Le Maire, M. (1997) *J. Biol. Chem. 272*, 17258−17262.
32. Andersen, J. P. (1994) *FEBS Lett. 354*, 93−96.
33. Andersen, J. P., and Vilsen, B. (1994) *J. Biol. Chem. 269*, 15931−15936.
34. Menguy, T., Corre, F., Bouneau, L., Deschamps, S., Moller, J. V., Champeil, P., Le Maire, M., and Falson, P. (1998) *J. Biol. Chem. 273*, 20134−20143.
35. Bastide, F., Meissner, G., Fleischer, S., and Post, R. L. (1973) *J. Biol. Chem. 248*, 8385−8391.
36. Degani, C., and Boyer, P. D. (1973) *J. Biol. Chem. 248*, 8222−8226.
37. Masuda, H., and de Meis, L. (1973) *Biochemistry 12*, 4581−4585.
38. Adams, P., East, J. M., Lee, A. G., and O'Connor, C. D. (1998) *Biochem. J. 335*, 131−138.
39. Guillain, F., Champeil, P., and Boyer, P. D. (1984) *Biochemistry 23*, 4754−4761.
40. Rice, W. J., and MacLennan, D. H. (1996) *J. Biol. Chem. 271*, 31412−31419.
41. Fernandez-Belda, F. J., Kurzmack, M., and Inesi, G. (1984) *J. Biol. Chem. 259*, 9687−9698.
42. Dupont, Y. (1982) *Biochim. Biophys. Acta 688*, 75−87.
43. Inesi, G. (1987) *J. Biol. Chem. 262*, 16338−16342.
44. Fabiato, A., and Fabiato, F. (1979) *J. Physiol. (Paris) 75*, 463−505.

BI000185M